

## Individual growth models support the quantification of isotope incorporation rate, trophic discrimination and their interactions

5 Sébastien Lefebvre<sup>1,\*</sup>, Marine Ballaud<sup>1</sup>, M. Teresa Nuche-Pascual<sup>1</sup>, Sarah Nahon<sup>2</sup>,

Rongsong Liu<sup>3</sup>, Carlos Martinez Del Rio<sup>4</sup>

<sup>1</sup>University of Lille, CNRS, ULCO, UMR 8187 LOG (Laboratory of Oceanography and Geosciences), Station marine de Wimereux, F-59000 Lille, France.

<sup>2</sup>INRAE, UPPA, UMR 1419, Nutrition, Métabolisme, Aquaculture, Université de Pau et des Pays de l'Adour, Saint Pée sur Nivelle, France

10 <sup>3</sup>Department of mathematics and statistics, University of Wyoming, Laramie, WY 82070, US

<sup>4</sup>Department of zoology and physiology, University of Wyoming, Laramie, WY 82070, US

\* [sebastien.lefebvre@univ-lille.fr](mailto:sebastien.lefebvre@univ-lille.fr)

15

20

25

30 Authors Contribution: SL, RL and CMR conceived and designed the study. SL, MB, and SN performed the results. All authors analyzed the results and wrote the manuscript.

## Abstract

Two large but independent bodies of literature exist on two essential components of the  
35 dynamics of isotopic incorporation: the isotopic incorporation rate ( $\lambda$ ) and the trophic  
discrimination factor ( $\Delta$ ). Understanding the magnitude of these two parameters and the  
factors that shape them is fundamental to interpret the results of ecological studies that rely on  
stable isotopes.  $\lambda$  scales allometrically with body mass among species and depends on growth  
within species. Both are often assumed to be constant and independent of each other but  
40 evidence accumulates that might be linked and to vary with growth. We built and analyzed a  
model (IsoDyn) that connects individual growth and isotopic incorporation of nitrogen into  
whole body and muscle tissues. The model can assume a variety of individual growth patterns  
including exponential or asymptotic growths.  $\lambda$  depends on the rate of body mass gains which  
scales allometrically with body mass.  $\Delta$  is a dynamic response variable that depends partly on  
45 the ratio between fluxes of gains and losses and covaries negatively with  $\lambda$ . The model can be  
parameterized either from existing large databases of animal growth models or directly from  
experimental results. The model was applied to experimental results on three ectotherms and  
one endotherm and compared to the results of the simpler and widely used time model.  
IsoDyn model gave a better fit with relatively little calibration. IsoDyn clarifies and expands  
50 the interpretation of isotopic incorporation data.

Key words : Stable isotopes; isotopic turnover rate; nitrogen; animal, trophic ecology

## 55 Introduction

Animal ecologists rely on stable isotope analysis (SIA) of carbon, nitrogen, and sulfur, to trace the pathways of organic matter through food webs, to estimate trophic position, to examine intra- and inter-species trophic relationships (i.e. niche properties), to track origins 60 and migration of animals, and to reconstruct animals' diets (reviewed by Boecklen et al. 2011, Glibert et al. 2018 or Shipley and Matich 2020). Most of these applications hinge on the observation that the isotopic value of animal tissues resembles that of their diet with a small difference (De Niro and Epstein 1978) called trophic discrimination factor (Healy et al. 2018) and denoted by a  $\Delta$  with ‰ units (see Table 1 for a list of symbols and their definitions). 65 However, many applications of SIA in trophic ecology depend on an additional observation: the incorporation of the value of resources into consumer's tissues after a diet change is not instantaneous, but obeys predictable temporal dynamics (Martinez del Rio and Carleton 2012). The isotopic incorporation rate ( $\lambda$  with units of time<sup>-1</sup>) is construed as the instantaneous rate of isotopic incorporation with the interpretation of  $1/\lambda$  as the average retention time of an 70 element in a tissue, and  $\ln(2)/\lambda$  as its half-life (Thomas et al. 2015; Vander Zanden et al. 2015).

Ecologists and physiologists have conducted large numbers of experiments that describe the temporal changes of the isotopic values in consumer's tissues after animals shift between 75 diets of different isotopic composition (the so-called diet switching experiments, DSE, Fry and Arnold 1982, Thomas et al. 2015; Vander Zanden et al. 2015). Often, these experiments have the dual objective of estimating both  $\lambda$  and  $\Delta$ . The results of these experiments are interpreted by fitting a family of 2 to 3 parameter models that assumes one-compartment, first order-kinetics and exponential growth of the consumers under study (e.g. Fry and Arnold 80 1982; Tieszen et al. 1983; Hesslein et al. 1993 and later on Carleton and Martinez Del Rio 2010). These models (referred here as isotope incorporation models, DIIM) have many virtues: they are simple, their parameters can be easily estimated and readily interpreted, and they provide an excellent fit to the temporal changes in the isotopic values of animals that 85 follow a diet change. For instance, the widely applied time model (Tieszen et al. 1983) follows:

$$\delta_t = \delta_\infty - (\delta_\infty - \delta_0)e^{-\lambda t} \quad \text{Eq(1)}$$

Where  $\delta_t$  is the isotopic composition of the consumer's tissues over time after a diet switch, 90  $\delta_\infty$  is the asymptotic value when tissues have reached steady state with the new diet ( $\delta_d$  i.e. isotopic equilibrium) for a given incorporation rate ( $\lambda$ ), and  $\delta_0$  is the isotopic composition of the consumer's tissues at the beginning of the DSE.  $\Delta$  is often estimated as a by-product of the estimation of  $\delta_\infty$ :

$$\delta_\infty = \delta_d + \Delta \quad \text{Eq(2)}$$

95

The value of  $\lambda$  can be partitioned into two components (Heisslein et al. 1993): the mass-specific growth rate ( $k_g$ ) that corresponds to the contribution of tissue addition due to growth and evaluated by an exponential model (with  $W$  the body mass, and  $W_0$  the initial body mass), and the catabolic turnover rate ( $k_c$ ) that corresponds to the replacement of existing tissue.

100

$$\lambda = k_g + k_c \quad \text{Eq(3)}$$

$$W_t = W_0 e^{k_g t} \quad \text{Eq(4)}$$

105

Equation 3 may not evaluate properly the contribution of  $k_g$  and  $k_c$  to  $\lambda$  when animal's growth does follow an exponential pattern. For instance, MacAvoy et al. (2005) experimented on young adult mice approaching their asymptotic body mass. They observed a steady decrease in  $k_g$  along the course of one DSE and estimated different  $k_g$  values at different times. This problem can be solved by recognizing that most animals follow common asymptotic growth patterns (Kearney 2020) such as described by the von Bertalanffy growth model (von Bertalanffy 1957), the DEB theory (Kooijman, 2010) or the ontogenetic growth model (West et al. 2001) in which true exponential growth occurs only during early life stages.

110

Many applications of SIA in trophic ecology assume both (1) an isotopic equilibrium between the isotopic values of consumers' tissues and its food sources (i.e. that  $\lambda$  is large at the time of measurement but see Marin Leal et al. 2008 and reference therein) and (2) a constant value of  $\Delta$  among individuals of a population and even among different species (Phillips et al. 2014).

115

These assumptions allows to a widely use of sophisticated user-friendly algorithms to solve mixing models that attempt to resolve a consumer's diet composition from the isotopic values of its tissues (e.g. Parnell et al.'s (2010) Bayesian mixing model, SIAR). The importance of  $\Delta$  values for the interpretation of ecological isotopic data, via mixing models, has led to compilation of large data sets of values and new methods to predict them (Healy et al. 2018).

120

Although some tantalizing patterns between tissue type (and thus amino acid composition and

isotopic incorporation), form of nitrogen excretion, nutritional status, and phylogeny have been documented (McCutchan et al. 2003; Vanderklift and Ponsard 2003; Healy et al., 2018), some of the drivers of differences in  $\Delta$  remain elusive (Caut et al. 2009).

125 More recently,  $\lambda$  has received new attention (as reviewed by Carter et al. 2019). The estimation of  $\lambda$  is crucial to determine the time window over which diet could be reconstructed (Dalerum and Angerbjorn 2005; Phillips et al. 2014) or to model ontogenetic diet shift (Hertz et al. 2016). Incorporation rate is also a component explaining part of the isotopic variance used to evaluate the trophic niche (Fink et al. 2012; Yeakel et al. 2016). In 130 fact,  $\lambda$  is a function of the body size and is expected to vary allometrically within species (Martinez Del Rio et al. 2009). This expectation has been proven to be correct between species (Thomas et al. 2015; Vander Zanden et al. 2015), even though the relationship between  $\lambda$  and body mass has large residual variation that remains unexplained. Assuming 135 isotopic equilibrium and a constant  $\Delta$  in isotopic ecology are possibly the result of our still incomplete understanding of the factors that shape their values: these strong assumptions should be relaxed.

Isotope ecologists have compiled large data sets of  $\lambda$  and  $\Delta$  values estimated using DSE interpreted with first-order one-compartment models (Eq 1, 2 and 3), and assuming that these two parameters are independent and constant over the course of one DSE. Nonetheless, 140 theoretical and empirical evidences suggest  $\lambda$  and  $\Delta$  are dynamic and linked. On the empirical side, Lefebvre and Dubois (2016) and Gorokhova (2018) documented strong negative relationships between  $\Delta^{15}\text{N}$  and  $k_g$  (which is the dominant determinant factor of  $\lambda$  in rapidly growing organism, Hesslein et al. 1993) in exponentially growing animals. Villamarín et al. (2018) documented a negative relationship between  $\Delta^{15}\text{N}$  of crocodiles and their  $k_g$  that could 145 not be accounted for a change in diet. On the theoretical side, the models of Olive et al. (2003) and Martinez del Rio and Wolf (2005) suggest a decreasing relationship between  $\Delta^{15}\text{N}$  and  $\lambda$ . The generality of this result is unknown because both Olive et al. (1999) and Martinez del Rio and Wolf (2005) modelled only the special case of animals growing exponentially. Pecquerie et al. (2010) constructed a more general approach (which is called Dynamic 150 Isotopic budgets DIB) that assume asymptotic growth. This approach combines an accounting of the fate of different elements on the body compartments defined by the dynamic energy budget theory (DEB, Kooijman 2010). Emmery et al. (2011) applied Pequerie et al. (2010)'s DIB approach to Pacific oysters (*Crassostrea gigas*) and found that  $\Delta^{15}\text{N}$  declined from 5 to 2

155 %o with increasing  $k_g$ . Like DEB-dependent growth models, DIB models are species-specific  
155 and each case requires calibration with a high number of parameters (over 22 in the case of  
Emmery et al.'s (2011) application), although DEB models can be potentially parameterized  
with values from a huge database (Marques et al., 2018). Moreover, their application involves  
computationally intensive calibration and expertise in DEB that is not common among  
ecologists. We venture that for this reason, Pecquerie et al.'s (2010) model has not been  
160 applied widely. As far as we know, Emmery et al. (2011)'s study is its only empirical  
application to stable isotope studies.

165 Our purpose is to construct a relatively simple mathematical model that allows researching  
the interplay between growth,  $\Delta$  and  $\lambda$  at the whole body and element levels while including  
other previous conventional models as special cases (Fig. 1). Our model permits exploring the  
hypothesis that  $\lambda$  and  $\Delta$  are neither constant nor species specific, but predictably variable  
among individuals and dynamically linked. We hypothesize that such model would be more  
accurate in describing incorporation dynamics than conventional models particularly when  
consumer growth deviates from pure exponential trajectories (early life stages). The dual  
170 assumption of constancy and independence between  $\lambda$  and  $\Delta$  precludes inferring their values  
for different life stages than the ones observed and estimated in DSEs. Another consequence  
of assuming static  $\Delta$  and  $\lambda$  within the course of DSEs would be an improper estimation of  
their values and potentially the contribution of  $k_g$  and  $k_c$  to  $\lambda$ . The relative simplicity of our  
model facilitates its parameterization. By constructing a model that can incorporate the many  
175 ways in which animal growth has been described (for example by the ontogenetic growth  
model (West et al. 2001; Hou et al, 2011), von Bertalanffy growth model (von Bertalanffy  
1957) and DEB theory (Kooijman 2010)), our model offers a new and dynamic perspective to  
interpret DSEs, but also provide a tool to help explain the still unexplained variation in  $\Delta$  and  
 $\lambda$ , and in doing so provide a conceptual link between trophic isotopic ecology and the study of  
180 animal growth and life histories.

## Methods

### IsoDyn as a new model of isotopic incorporation

185 Although our model is general enough to be used by all of the stable isotopes commonly used  
in ecological research (C, N, S, H, and O), we will focus on nitrogen (N). The isotopic value

of this element ( $\delta^{15}\text{N}$ ) and its trophic discrimination factor ( $\Delta^{15}\text{N}$ ) are used to estimate trophic position, and thus  $\Delta^{15}\text{N}$  has been relatively well studied (Post 2002; Glibert et al. 2019). Further, dietary protein is assumed to be the main driver of  $\delta^{15}\text{N}$  incorporation rate and  $\Delta^{15}\text{N}$  is less sensitive to isotopic routing than  $\Delta^{13}\text{C}$  (Martinez Del Rio et al., 2009).

We assume here that body mass dynamics ( $W_t$ ) of a consumer follows an asymptotic growth pattern (see supplementary material 1 for details), giving:

$$W_t = \left\{ W_\infty^{1-\beta} + (W_0^{1-\beta} - W_\infty^{1-\beta}) e^{-r_o(1-\beta)t} \right\}^{\frac{1}{1-\beta}} \quad \text{Eq(5)}$$

195 with

$$\lim_{t \rightarrow \infty} W_t = W_\infty = \left( \frac{r_i}{r_o} \right)^{\frac{1}{1-\beta}} \quad \text{Eq(6)}$$

and with

$$k_g = \frac{1}{W} \frac{dW}{dt} = r_i W_t^{1-\beta} - r_o \quad \text{Eq(7)}$$

200 where  $r_i$  and  $r_o$  are rates of gains and losses respectively (assimilation and excretion in the case of N),  $\beta$  the allometric coefficient and  $W_\infty$  is the asymptotic body mass.

Under these body mass dynamics,  $\delta^{15}\text{N}$  values in a consumer tissues follows (see supplementary material 1 for details) :

$$\frac{d\delta^{15}\text{N}}{dt} = r_i W^{\beta-1} (\delta^{15}\text{N}_d - \delta^{15}\text{N} + \Delta_i) - \Delta_o r_o \quad \text{Eq(8)}$$

where  $\Delta_i$  and  $\Delta_o$  are discrimination factors on gains and losses respectively.

Eq(8) is a linear differential equation without a general analytical solution when  $\beta$  is lower than 1 (i.e. for asymptotic growth models such as the von Bertalanffy model). However, a 210 discrete approximation can be done for small  $dt$ :

$$\delta^{15}\text{N}_{t+1} = \delta^{15}\text{N}_\infty - (\delta^{15}\text{N}_\infty - \delta^{15}\text{N}_t) e^{-r_i W_t^{\beta-1} dt} \quad \text{Eq(9)}$$

This approximation of Eq(8) then parallels the time model in Eq(1), most commonly used to 215 describe and interpret isotopic incorporation data in DSEs, but with  $\delta^{15}\text{N}_\infty$  and  $\lambda$  depending on the body mass at time  $t$ :

$$\delta^{15}N_\infty = \delta^{15}N_d + \Delta^{15}N_t \text{ with } \Delta^{15}N_t = \Delta_i - \frac{\Delta_o r_o}{r_i W_t^{\beta-1}} \quad \text{Eq(10)}$$

and

220  $\lambda_t = r_i W_t^{\beta-1} = k_g + r_o \quad \text{Eq(11)}$

Eq(10) and eq(1) differ between them in that the terms equivalent to  $\delta^{15}N_\infty$  and  $\lambda$  (eq(2) and eq(3) vs eq(10) and eq(11) respectively) vary with time. Another difference is that partitioning between growth and catabolism is variable in eq(11) because  $k_g$  is variable while it was constant in eq(3) due to the assumption of exponential growth (eq 4). Note that  $r_o$  is equivalent to  $k_c$  or  $m$  in eq(3). These equations highlight the predictable dependence of  $\lambda$  and  $\Delta^{15}N$  on the parameters that shape growth ( $\beta$ ,  $r_i$  and  $r_o$ ). A large number of studies report values for these parameters (see e.g. West et al. 2001 for the ontogenetic growth model; and Kooijman 2010 for von Bertalanffy 1957). Eq(8) also means that the isotopic incorporation rate for N can be estimated from the dynamics of body mass as long as the proportion of N in 230 the body mass ( $p_N$ ) is constant (see supplementary material 1 for explanations). This important feature applies to any pool of element as for instance carbon or sulfur in the absence of isotopic routing.

### Simulations and parameter estimations

235 One of the major advantages of our model is that it can be parameterized and fitted readily with available information data or data that can be gathered in DSE. Describing dynamics of body mass require three parameters that are  $r_i$ ,  $r_o$  and  $\beta$ , and only two parameters if we consider  $\beta$  following a common framework (e.g.  $\beta=2/3$  in the case of the von Bertalanffy growth model). Two additional parameters are needed,  $\Delta_i$  and  $\Delta_o$ , for simulating the 240 incorporation dynamics of stable isotopes. Simulations presented here, were generated following a numerical integration algorithm under R software v.4.0.3 (2019) using the package DeSolve (Soetaert et al. 2010) to solve eq (8). Because fitting the four parameters ( $r_i$ ,  $r_o$ ,  $\Delta_i$  and  $\Delta_o$ ) from data on isotope incorporation alone ( $\delta^{15}N$  values over time) is not possible, the parameters can be estimated in two ways which can be called simultaneous and 245 sequential and by using dynamics of body mass in parallel.

In simultaneous estimation, the parametrization of the four main parameters ( $r_i$ ,  $r_o$ ,  $\Delta_i$  and  $\Delta_o$ ) can be done using both the dynamics of body mass and stable isotopes incorporation. For simplicity, we chose to perform the calibration considering that  $\Delta_i$  and  $\Delta_o$  as opposite values

but equal in absolute value ( $\Delta_i = -\Delta_o$ ). This means that the same isotopic discrimination was  
250 applied to gains and losses, an assumption also done by Flynn et al (2018) in a mechanistic simulation model. Parameter estimations were performed using the Nelder Mead function of the lme4 package which allows to set boundaries for the parameters ( $r_i$  and  $r_o$  must be positive). The function minimizes the sum of two symmetric bounded loss functions (hereafter named the cost function) which accounts for the difference between predictions and  
255 observations for dynamics of body mass and stable isotopes respectively. This cost function is ideally suited to fit several models to several dataset (Marques et al. 2019). Local minima can be found during the optimization process. In order to ensure to detect the global minimum, the initial starting values of the parameters were randomly selected and the procedure is performed twice first (N=2). Then, the process continues (up to N=20) until the value of the  
260 cost function for the last set of parameters is lower than the best set by 5%. Parameter sets in which some parameters stuck to the boundaries were systematically deleted. Interval estimates of parameters were evaluated using a bootstrap method (N=500) by adding log-normally distributed scatter (mean coefficient of variations of observations) to the predictions with replacement of the original data sets (Marques et al. 2019). We then compare the  
265 parameters of the IsoDyn model with the time model partitioning  $\lambda$  into  $k_g$  and  $k_c$  (eq 1, 2, 3 and 4). The time and exponential models were fitted with the nls2 package. Goodness of fit of all the models was assessed by the relative error (RE) as calculated by Marques et al. (2019):

$$RE = \sum_{i=1}^N \frac{|p_i - d_i|}{|d_i|} \quad \text{Eq(12)}$$

where  $p_i$  and  $d_i$  are prediction and observation, respectively, for a given data point  $i$  and  $N$  is  
270 the total number of data points.

The sequential estimation consists first in obtaining estimates for  $r_i$  and  $r_o$ , which allows estimating body mass over time as well as  $\lambda$ . This can be done either by conducting experiments and fitting the parameters of von Bertalanffy (1957) or West et al. (2001)'s  
275 equations. In the absence of sufficient experimental data,  $r_i$  and  $r_o$  can be obtained from data bases developed from DEB theory such as “Add my Pet” (Marques et al., 2018) or the ontogenetic growth model (West et al. 2001; Hou et al. 2011) or studies on the selected species. Then, the estimation of  $\Delta_i$  and  $\Delta_o$  were done in a second step by implementing the values of the three previous parameters in Eq (8).

280 R code for all analyses, figures and tables is available from GitHub  
(<https://github.com/Sebastien-Lefebvre/IsoDyn>)

### Data sets

For our model to be calibrated or validated, dynamics of body mass in parallel to dynamics of nitrogen stable isotope incorporation are needed and these combinations are not often reported  
285 in experimental studies. Our predictions apply to the whole organism. However, it is generally assumed that muscle tissue and other structural tissues form the majority of an organism's body mass and that consequently isotopic dynamics of the whole organism can be approximated by the ones of muscle tissues (Thomas and Crowther 2015). We have then  
290 selected four studies to highlight the different ways to estimate parameters in the context of DSEs. The first study applied on young adult mouse (*Mus musculus*) approaching the maximum body mass (MacAvoy et al., 2005). Stable isotope incorporation dynamics were measured over 112 days DSE on skeletal muscle ( $\delta^{15}\text{N}_m$ ) using an experimental diet. *Mus musculus* is a small endotherm species with a maximum body mass of ca 25 g. In the second  
295 study, Pacific yellowtail (*Seriola lalandi*) juveniles were used for a 98 days DSE in which incorporation dynamics of stable isotope ratios of nitrogen of dorsal muscle ( $\delta^{15}\text{N}_m$ ) were measured (Nuche -Pascual et al. 2018). Fish were fed with a commercial diet. *Seriola lalandi* is a large ectotherm species with a maximum body mass of ca 193 kg. In the third study, sand goby (*Pomatoschistus minutus*) late juveniles were used for a 90 days DSE and  $\delta^{15}\text{N}_m$  values  
300 were measured (Guelinckx et al. 2007). Fish were fed with a commercial diet. *Pomatoschistus minutus* is a small ectotherm species with a maximum body mass of ca 7 g. These three first studies were calibrated following the simultaneous estimation. In the fourth and last study, the growth rate of common carp (*Cyprinus carpio*) was manipulated by changing food availability providing four different diet switching experiments lasting eight weeks (Gaye -  
305 Siesssenger et al. 2004). Only start and end values of body mass and  $\delta^{15}\text{N}$  values of the whole body ( $\delta^{15}\text{N}_b$ ) were originally provided for this study. *Cyprinus carpio* is a medium ectotherm species with a maximum body mass of ca 40 kg. This last study was calibrated using the sequential method for estimates of  $r_i$  and  $r_o$  of this species as described by the DEB theory (ESM 2).

310

### **Results**

Although our model shares a variety of characteristics with previous models, it has specific ones. In this section we highlight two of those: 1) IsoDyn model makes explicit links between

315 growth and isotopic incorporations patterns; 2) the model allows parameterizing and fitting existing patterns on the dynamics of isotopic incorporation particularly when consumer growth deviates from pure exponential trajectories. Before considering our analyses on the four case studies, we considered a few general traits of our model that distinguishes it from previous ones.

320

### Growth and isotopic incorporation patterns are predictably linked

325 Our model predicts that the relationships between body mass and the isotopic value of tissues such relationships and their effects on body mass,  $\lambda$  and  $\delta^{15}\text{N}$  dynamics are given in Fig. 2 for three virtual species characterized by different values and ratios of  $r_i$  and  $r_o$ , a common  $\beta=2/3$  and initial body mass  $W_0=0.1$  g. Species 1 (Sp1) and species 2 (Sp2) have the same asymptotic body mass ( $W_{\max}=64$  g eq(7)) but differ in their mass gains and losses rates by half ( $r_{i1}=0.2$  g<sup>1/3</sup> d<sup>-1</sup>,  $r_{o1}=0.05$  d<sup>-1</sup>,  $r_{i2}=0.1$  g<sup>1/3</sup> d<sup>-1</sup>,  $r_{o2}=0.025$  d<sup>-1</sup>). As rate of losses ( $r_o$ ) governs the steepness at which  $W_{\max}$  is reached, Sp1 reached its  $W_{\max}$  faster (Fig. 2A). Species 3 has higher  $r_{i3}=0.6$  g<sup>1/3</sup> d<sup>-1</sup> and  $r_{o3}=0.2$  d<sup>-1</sup> but lower  $W_{\max}=27$  g. Dynamics of isotopic incorporation are then explained by two components,  $\lambda$  and  $\delta^{15}\text{N}_{\infty}$  value which are both dynamic in our model (see equation 10 and 11).

335 Typically,  $\lambda$  decreases over time along with body mass. On a ln/ln scale, the slope is negative and equals  $\beta-1$ , and the intercept is  $\ln(r_i)$  (Fig. 2B);  $r_i$  and thus  $\lambda$  are higher in Sp3 than Sp1 and Sp2. The range of  $\lambda$  displayed by one species depends on the difference between  $W_0$  and  $W_{\max}$ , which is lower for Sp3. As  $\lambda$  and  $k_g$  decrease,  $\delta^{15}\text{N}$  difference between body and diet ( $\delta^{15}\text{N}_b - \delta^{15}\text{N}_d$ ) increases (Fig. 2C). When growth approaches zero,  $\delta^{15}\text{N}$  dynamics are 340 dominated by flux of body mass losses (i.e. excretion) and  $\delta^{15}\text{N}_b - \delta^{15}\text{N}_d$  reaches its maximum (i.e.  $\Delta_i - \Delta_o = 4\%$ ). On the opposite, when growth tends to its maximal value,  $\delta^{15}\text{N}_b - \delta^{15}\text{N}_d$  approaches  $\delta^{15}\text{N}_d$  (here set at 0) and  $\delta^{15}\text{N}$  dynamics are dominated by the flux of mass gains (i.e. assimilation). The inflection characterizes the trade-off between fluxes of gains and losses dominance in  $\delta^{15}\text{N}$  dynamics. Then, the range of these values depends on the extent of  $k_g$  345 performed by the species between initial body mass (i.e. birth  $W_0$ ) and  $W_{\max}$ . These results suggest that the  $\delta^{15}\text{N}$  dynamics obtained in DSE will depend on the stage of growth at which experiments are done. Typical DSEs were performed using features of the

three species above at two life stages (juveniles i.e. from  $W_0$  and adult at  $W_{max}$ ). As our analysis of special cases indicates,  $\delta^{15}N_b$ -  $\delta^{15}N_d$  values will be lower in experiments involving 350 organisms growing in the early, quasi-exponential, phases of body growth than in animals of the same species that have reached or are close to the asymptotic body mass.

In Sp1 and Sp3, adults reach the asymptotic isotopic composition faster, because  $\lambda$  (which equals  $r_o$  in adults) remains quite high even for adult while  $\delta^{15}N_b$ -  $\delta^{15}N_d$  is maximum (Fig. 3). 355 For the young of these species, although  $\lambda$  is even higher than for adults,  $\delta^{15}N_b$ -  $\delta^{15}N_d$  is still increasing and this prevents from reaching fully the asymptote for juveniles of Sp1. The pattern is a bit different for Sp2 (Fig. 3). As juveniles of Sp2 are still performing high  $k_g$ , then  $\lambda$  remains high and the  $\delta^{15}N_b$ -  $\delta^{15}N_d$  although increasing, is still low: asymptotic isotopic composition remains a moving target and cannot be fully reached. In Sp2 adults,  $\lambda$  is twice 360 lower than for Sp1, and its value does not reach the asymptotic value within the 100 days of the experiment.

#### Case study: calibration using the simultaneous parameter estimation

The three species studied are an endotherm (the house mouse *Mus musculus*) and two 365 ectotherms (the two fish species Pacific yellowtail, *Seriola lalandi* and sand goby, *Pomatoschistus minutus*), at different life stages and as a consequence, in different growth situations at the time of DSE. The young adult mice approached their asymptotic body mass so that their growth rate gradually decreased during the experiment. The mouse body mass gain was about 25% (Fig. 4). Individuals of both fish species were juveniles and showed a 370 linear body mass increase for Pacific yellowtail and an exponential increase for sand goby with a body mass gain of 600% and 100% respectively (Fig. 4).

A comparison between the conventional isotopic incorporation time model and IsoDyn model was done. Both models displayed very good and comparable goodness of fit concerning  $\delta^{15}N$  375 values (as estimated by the RE Table 2). However, the two models differed strongly in the prediction of body mass dynamics for two species (mouse and Pacific yellowtail) which did not follow exponential growth patterns. In these two cases, the exponential model fitted poorly to the data whereas IsoDyn model fitted better. Both models displayed a very good fit for sand goby growing exponentially. Therefore, IsoDyn model performed better than the

380 time model regarding simultaneously the body mass and  $\delta^{15}\text{N}$  dynamics (mean RE Table 2) when body mass dynamics did not follow an exponential pattern.

The estimated parameters were of the same order of magnitude for both models but in some cases they differed substantially, especially for  $\lambda$ ,  $k_g$  and  $k_c$  (Table 2). The estimates of  $\Delta$  values were roughly the same in both models, although slightly higher in the case of IsoDyn model (10 to 20% for sand goby and Pacific yellowtail, respectively).  $k_g$  were identical in the case of sand goby and smaller for the two other species which body mass dynamics deviated from the exponential pattern.  $\lambda$  estimates were comparable for the first two species (mouse and Pacific yellowtail) but it was 60% smaller using IsoDyn model compared to the time model for the sand goby. As a result, the proportion of  $k_g$  explaining  $\lambda$  differed noticeably from one case to another. In mouse and Pacific yellowtail,  $k_g/\lambda$  ratios were 10 to 20% lower respectively in IsoDyn estimates, whereas it was 60% higher for the sand goby. As for the specific estimates of the IsoDyn model,  $r_i$  ranked according to the maximum body mass of the species (Pacific yellowtail > mouse > sand goby) and  $r_o$  was higher for mouse (endotherm species). The predicted maximum body masses (as calculated with eq(7)) were 331.5 g, 23.5 g and 15.5 g for Pacific yellowtail, mouse and sand goby respectively. Isotopic discrimination on assimilation or excretion rates ( $\Delta_i$  and  $\Delta_o$  respectively) ranged from 0.8 to 2.1 %. The strong interplay of growth and isotopic incorporation dynamics in IsoDyn model offer new perspectives in the interpretation of  $\lambda$  and  $\Delta$  and a more consistent evaluation of the contribution of growth and catabolic rates in  $\lambda$ .

#### Case study: calibration using the sequential parameter estimation

To determine the suitability of IsoDyn model when intra-specific variations of  $r_i$  and  $r_o$  occurs due to different ration levels, we re-analyzed the data from Gaye Siesssger et al. (2004). In 405 this DSE, the growth of Common carp (*Cyprinus carpio*) was manipulated by changing food availability through different feeding levels. We estimated parameters in a sequential approach because dynamics of body mass were restricted to start and end values preventing a reliable calibration of  $r_i$  and  $r_o$ . First, we used parameters from the DEB “Add My Pet” data set to calibrate the model (see supplementary material 2 for more details), and then adjusted 410 the scaled functional response ( $f$ ), an Holling type II function ranging from 0 to 1, that controls the rates of body mass gains ( $r_i$ ) and of body mass losses ( $r_o$ ) to fit the observations of

body mass change over time (Fig. 5). The  $f$  values were estimated to be 0.16, 0.29, 0.53, 0.82 from the lowest feeding ration levels to the highest ones (Table 2). This allowed estimating values of  $r_i$  and  $r_o$  for the four treatments according to ESM2 (Table 3). Then, independent 415 values of  $\Delta_i$  and  $\Delta_o$  were simultaneously fitted using  $\delta^{15}\text{N}_b$ -  $\delta^{15}\text{N}_d$  values and giving  $\Delta_i = 1.08\text{\textperthousand}$  and  $\Delta_o = -1.32\text{\textperthousand}$ . The model not only predicted the qualitative decrease of  $\delta^{15}\text{N}_b$ -  $\delta^{15}\text{N}_d$  values with  $k_g$  (Fig. 5) but, in addition, it yielded a very good quantitative fit to the data.

## Discussion

420 The IsoDyn model links growth and dynamics of isotopes incorporation

Existing dynamic models of isotope incorporation (DIIM) can be ranked in a continuum that spans from simple phenomenological models with few parameters (e.g. Fry and Arnold 1982; 425 Tieszen et al., 1983) to complex mechanistic models with many parameters (e.g. Pecquerie et al. 2010; Poupin et al. 2014). The first models developed were function of either body mass (Fry et al., 1982) or time (Tieszen et al., 1983). Each of these models was then improved later (Carleton and Martinez del Rio, 2010, Heisslein et al., 1993 respectively) in order to partition the  $\lambda$  into two components,  $k_g$  and  $k_c$ . As these improved models need an independent 430 estimation of  $k_g$ , they do not explicitly connect the underlying mechanisms common to both isotopes and body mass dynamics such as rate of mass gains ( $r_i$ ) and rate of mass losses ( $r_o$ ). Further, parameters from previous models are constant with time and body mass dynamics are restricted to the exponential or the steady state cases. However, they are simple to use and 435 describe experimental available data sets well in most cases, and have interpretable parameters but they are limited in that they can hide important details of the factors that shape the process of isotope incorporation in a dynamic way.

IsoDyn model renders  $\lambda$  dynamic by considering common and explicit parameters ( $r_i$ ,  $r_o$  and 440  $\beta$ ) to both  $\delta^{15}\text{N}$  and body mass dynamics, and offers the possibility to reproduce different growth patterns over the organism life span. This highlights a first important feature of the new model over the previous ones. A second important property of IsoDyn is the possible temporally variable trophic discrimination factor ( $\Delta^{15}\text{N}$ ) due to its interaction with growth. Our model allows for this interaction thanks to two fluxes of which the flux of gains is 445 allometrically related to body mass, plus that each of the fluxes being associated with a

445 discrimination value. Actually,  $\Delta^{15}\text{N}$  varies over time along with growth only if the  
discrimination linked to body mass losses ( $\Delta_0$ ) is different from zero (and most probably  
below zero). Interaction between  $\Delta^{15}\text{N}$  and growth was evidenced in experimental results (e.g.  
Lefebvre and Dubois 2016; Gorokhova 2018) and predicted by earlier mechanistic models but  
for the exponential case only (Olive et al. 2003; Martinez Del Rio et al. 2005). This  
450 interaction is absent in the conventional models developed earlier. IsoDyn model has the time  
model as a special case (i.e. when  $\lambda$  and  $\Delta^{15}\text{N}$  are constants,  $\beta=1$  and  $\Delta_0=0$ ) and shares with it  
ease of computation and analytical tractability.

455 Our model provides also a new link between models that describe isotopic incorporation  
phenomenologically and those that incorporate more mechanistic details. Pecquerie et al.  
(2010) and Emmery et al. (2011) applied dynamic energy budget theory (DEB) to clarify the  
processes that determine both  $\lambda$  and  $\Delta^{15}\text{N}$  values in an approach called Dynamic Isotope  
Budget modeling (DIB). Unlike our model, DIB models cannot be summarized simply as they  
are assumption-rich (Pecquerie et al. 2010). DIB recognizes the dynamic dependence of  
460 isotope incorporation dynamics on body mass and growth (Emmery et al. 2011). The results  
of DIB are consistent with our simpler mechanistic model. However, DIB is a two sequential  
compartments and three fluxes model at least, and then  $\Delta^{15}\text{N}$  is not only explained by the  
isotopic discrimination on fluxes but the proportion of the two sequential compartments that  
account for the body mass of organisms (i.e. reserve and structure compartments, Pecquerie et  
465 al. 2010; Lefebvre and Dubois 2016). In another approach, Poupin et al. (2014) developed a  
detailed mechanistic multi-compartment model of nitrogen pool and fluxes (21 compartments  
and 49 fluxes) on adult rat. They showed for instance a deviation from optima in food quality  
or quantity led to an increase of  $\Delta^{15}\text{N}$  at the whole body scale. Unlike IsoDyn model, DIB and  
the multi-compartment model demand detailed parameterization. The model that we describe  
470 shares some of the powerful characteristics of DIB or the multi-compartmental model while  
making it consistent with the mass-balance models more widely used by isotopic ecologists.

#### Parameterizing the model and the experiments that we need

475 Because growth is a central feature of an animal's ecological traits, IsoDyn model allows  
linking patterns of isotopic incorporation and trophic discrimination factor with the biology of  
animal life histories. This true link between growth and isotope incorporation offers several

possibilities regarding the parametrization of our model in simultaneous and sequential estimations: calibration of body mass dynamics and of dynamics of isotope incorporation  
480 could insight from each other.

The simultaneous approach allows strengthening the parametrization by coupling body mass dynamics and isotope incorporation dynamics into a single calibration procedure. The limit of this procedure stands in the number of parameters to be estimated since the higher the number  
485 of parameters, the bigger the problem of multiple local minima in the minimisation of the cost function. Specifying some parameters is then necessary to relax this problem. This was performed by assuming a known  $\beta$  (here  $\beta=2/3$ ), and that the two isotopic discrimination were equal in absolute values ( $\Delta_i = -\Delta_o$ ). Fittings were then very good. The rate of body mass gains ( $r_i$ ) ranked with maximal body size and this is coherent with metabolic theories (West et al.  
490 2001; Kooijman 2010). Estimates of  $r_i$  and  $r_o$  allow to predict the maximum body masses that can be reached by the three species using eq(6). The maximal body mass was correctly estimated for mouse (23.5 g vs 25 g) and sand goby 15.5 g vs 7 g) but was underestimated for Pacific yellow tail (331.5 g vs 193 kg) probably due to sub-optimal experimental conditions for this large and migratory fish species.

495 One way to improve the estimation of IsoDyn model parameters in the simultaneous estimation is to perform DSE with different conditions of growth for the same species fed with the same diet with measurement of body mass dynamics in parallel. It can be done performing either DSEs at different life stages of the same species with the same diet to  
500 satiation, or DSEs at different food rations at one life stage when growth is still significant. To our best knowledge, the first case has not been reported yet in literature. The second one is rare and the body mass dynamics with an adequate time resolution were not reported (e.g. Gaye Siesssenger et al. 2004; Lefebvre and Dubois 2016; Gorokhova 2018;). Unfortunately, most of DSEs reporting both body mass and  $\delta^{15}\text{N}$  dynamics used diets that differ in quality  
505 and are fed to satiation (Nahon et al. 2020), and this leads to different growth rates but possibly confounding results with additional sources of  $\lambda$  and  $\Delta^{15}\text{N}$  variations (e.g. diet type, mode of nitrogen excretion, etc...).

510 In the sequential parameter estimation, the model's simplicity allows ready parameterization with available estimates of  $r_i$ ,  $r_o$  and  $\beta$  (Common carp case study). Because our new model

incorporates widely used individual growth models, it links isotopic ecology with large bodies of data (Ontogenetic growth model, West et al. 2001; Hou et al. 2011, von Bertalanffy models, including DEB's "Add My Pet" data base and other growth rate data available for a large number of animals, Marques et al. 2018). The two approaches can explore the effect of food restrictions on body mass dynamics (Kearney 2020). Once the individual growth model is parameterized, calibrations of isotopic discriminations on flux of body mass gains and losses ( $\Delta_i$  and  $\Delta_o$  respectively) can be easily performed. Results from the Common carp case study have emphasized that  $\Delta_i$  was a bit lower than  $\Delta_o$ . The latter is probably the main driver of  $\Delta^{15}\text{N}$  enrichment in animal tissues (Poupin et al. 2014).

515 The range of values of  $\Delta_i$  and  $\Delta_o$  can be predicted from the relationship between  $\Delta^{15}\text{N}$  and  $k_g$ : When  $k_g$  is high for a given species  $\Delta^{15}\text{N}$  is mostly explained by  $\Delta_i$  whereas when  $k_g$  approaches 0,  $\Delta^{15}\text{N}$  equals  $\Delta_i - \Delta_o$ . For example,  $\Delta^{15}\text{N}$  varied between 2 and 4‰ depending on  $k_g$  in mysids (Gorokhova 2018), from 3 to 9‰ in invertebrates (Lefebvre and Dubois 2016), from 2 to 5‰ in a bivalve (Emmery et al., 2011) from 1 to 1.7‰ in the Common carp 525 case study (Gaye-Siesseger et al. 2004). From these ranges, one can predict that the  $\Delta_o$  values are probably higher than  $\Delta_i$  values in general. Generalizing the calibration of IsoDyn model on DSEs would help determine the range of the  $\Delta_o$  and  $\Delta_i$  values using meta-analyses on some particular taxons. Finally, a common problem in the interpretation of isotopic data from studies is that the family of eq(1) needs a DSE data set with a clear shift and a clear asymptote 530 to relax as much as possible the co-variation of  $\lambda$  and the asymptotic value ( $\delta_\infty$  needed to estimate  $\Delta^{15}\text{N}$ ) and their uncertainties. Our model relaxes the necessity of perfect DSEs since the calibration can be sequential. DSEs (e.g. Logan and Lutcavage 2010) that provide limited information for  $\lambda$  and  $\Delta^{15}\text{N}$  could be then exploited with the IsoDyn model used as an alternative.

535

### Implications of the IsoDyn model for isotopic ecology

With all its simplifying assumptions, the IsoDyn model represents significant progress. In particular, it offers new perspectives in understanding the variabilities of  $\lambda$  and  $\Delta^{15}\text{N}$  values, 540 two critical variables for the interpretation of isotopic data (Martinez del Rio et al. 2012). Vander Zanden et al (2015) or Thomas et al. (2015) constructed allometric relationships that relate  $\lambda$  values with body size and several authors have summarized data on  $\Delta^{15}\text{N}$  and searched for the potential causes for its variation (Vanderklift and Ponsard 2003; Caut et al.

2009; Healy et al. 2018). The allometric studies of Vander Zanden et al. (2015) and Thomas  
545 et al. (2015) verified the prediction that  $\lambda$  varies as an allometric function of body mass  
(Martinez del Rio et al., 2009). Although these relationships are in broad agreement with  
predictions, they have large residual variation that limits precise estimation. We hypothesize  
that some of this variation can be explained by growth, the factor identified by IsoDyn model  
as a major determinant of  $\lambda$  and  $\Delta^{15}\text{N}$ .

550 By necessity, these large comparative data sets gloss over the characteristics of the animals  
that might generate variation in  $\lambda$  and  $\Delta^{15}\text{N}$  due to growth. For example, the vast majority of  
the estimates of  $\lambda$  and  $\Delta^{15}\text{N}$  on endotherms with determinate growth like birds and mammals  
are done on fully-grown adults. The same is the case of measurements of small invertebrates  
555 that reach asymptotic body mass in a short time. In contrast, experiments on ectotherms with  
indeterminate growth such as fish, amphibians, and reptiles are done in growing juvenile  
animals. This growth effect may explain why  $\Delta^{15}\text{N}$  mean values in ectotherms are slightly  
lower than the ones on endotherms (Caut et al. 2009). Re-analysing results of these meta-  
analyses using the IsoDyn model would be an interesting perspective. Further, we identified  
560 areas in which its application can solve long-standing questions to merge isotopic ecology and  
trophic ecology more seamlessly: the reconstruction of diet, the interpretation of “isotopic  
niches” and the determination of trophic level and food web structure.

565 Stable isotopes are very often used within mixing models to estimate the proportions of  
dietary items with contrasting isotopic values into animal diets at species (Layman et al.  
2012) and food web level (see Kadoya et al. 2012). Indeed the use of mixing models to  
estimate diet proportions has increased exponentially over the last years (as referred to in the  
citation dynamics of Parnell et al. 2010 paper). The mixing models used for this purpose  
require estimates of  $\Delta^{15}\text{N}$  and assumed isotopic equilibrium between diet and consumers.  
570 Relaxing the isotopic equilibrium assumption has been the concern of several studies with  
different prospects but in which the Isodyn model may help to quantify the parameter values.  
Phillips et al. (2014) recommended to carefully consider the time period over which the  
putative food sources have to be sampled to back calculate diet using mixing-models.  
Actually, this time period relies on  $\lambda$  (Thomas and Crowther 2015). Stock and Semmens  
575 (2016) integrated a new component in their mixing models by accounting for the variation in

consumption rate between individuals of a population. The rate of body mass gains ( $r_i$ ) is a proxy of this consumption rate.

Hertz et al. (2016) evidenced that  $\lambda$  is a critical parameter when modelling ontogenetic diet shifts. They typically modified a growth incorporation model in which  $\lambda$  vary with the body mass increase (Fry and Arnold 1982), but they kept constant the contribution of  $k_g$  and  $k_c$  while it is variable in the IsoDyn model. Finally, many ecologists analyse muscle for large species or whole body for small species, those working on endotherms use blood, and paleontologists are constrained to the analysis of bone and collagen. These tissues have widely different  $\lambda$  values (Thomas and Crowther 2015) and can have different  $\Delta^{15}\text{N}$  within an organism (Vanderklift and Ponsard 2003). A multi-compartment extension of the Isodyn model might allow predicting the magnitude of  $\Delta^{15}\text{N}$  values among tissues and the effect of growth on these values. Building a multi-compartment extension of the IsoDyn model has both computational and empirical challenges. Martínez del Rio and Andreson-Sprecher (2008) described how to arrange several compartments in parallel or sequentially (or a mix of both as in DIB for adults) but the model used assumes steady state or exponential growth and like all conventional models it assumes no dynamic pattern for  $\lambda$  and  $\Delta^{15}\text{N}$ . Unlike Poupin et al.'s (2014) model which assumes that the animals are not growing and hence allows using a system of linear differential equations, the multi-compartment Isodyn model is non-linear and hence is computationally more complex. Furthermore, the model requires empirical data of changes in fluxes among compartments that can vary in relative size during development or not. Challenging as they will be, these models are needed to estimate observed differences in both  $\lambda$  and  $\Delta^{15}\text{N}$  in different organs.

Our model suggests that differences in  $k_g$  can distort the geometry of isotopic niches beyond the frequency of diet change (Yeakel et al. 2016). The characteristics of the space occupied by individuals, populations, and by species assemblages in isotopic space are often used to interpret trophic structure (Shipley and Matich 2020). For example, the area of standard ellipses (and other metrics of extent of occupancy of isotopic space, Layman et al. 2012) is often used to assess variation in resource use (Parnell et al. 2013). Gorokhova (2018) demonstrated experimentally that the characteristics (as assessed by commonly used metrics) of the “isotopic niches” were dependent on growth (and hence on feeding regime) in Mysid shrimp (*Neomysis integer*) fed on the same food but different rations. In accordance with the

results of IsoDyn model, she found lower  $\Delta^{15}\text{N}$  in animals fed at high rations and hence  
610 growing more rapidly. Through its effects on  $\lambda$  and  $\Delta^{15}\text{N}$ ,  $k_g$  can change the position and variance (as measured by area occupied in isotopic space) of isotopic niches all the more so as growth is time dependent. The interpretation of isotopic patterns must be informed by the mechanisms that shape them, including growth rate.

615 The value of  $\Delta^{15}\text{N}$  is not only used in mixing models applied to determine diet composition. It is also often used to estimate an animal's trophic position in a food web (Post 2002; Quezada -Romegialli et al. 2018). An extension of this application is the use of the interspecific range of  $\Delta^{15}\text{N}$  values in assemblages of consumers to estimate the length of a food chain (Vander Zanden and Fetzer 2007). The prediction of our model adds a note of caution to the  
620 interpretation of the use of stable isotopes as estimates of trophic position and food-chain length, but opens the opportunity to make these measurements more accurate. Villamarín et al. (2018) identified a clear mismatch between trophic position estimated from  $\Delta^{15}\text{N}$  measurements and diet in crocodiles. This mismatch was largely explained by a decrease in  $\Delta^{15}\text{N}$  with  $k_g$  consistent with the predictions of the IsoDyn model (Villamarín et al. 2018).

625 The often reported positive correlation between  $\Delta^{15}\text{N}$  and body size in fishes (e.g. Nakazawa et al. 2010) that is attributed to upwards shifts in trophic position might have to be reconsidered in light of declining growth rates (and hence  $\Delta^{15}\text{N}$  values) with size predicted by our model. This could also have additional unsuspected consequences when scaling  $\delta^{15}\text{N}$  values and trophic level (Hussey et al. 2014).

630 So far, patterns of occupancy in isotopic space are used to infer the ecological characteristics of individuals, populations, and food web structure. Our model suggests that patterns in measured isotopic values are not only the result of a one-way translation of resource use into isotopic value. They are the dynamic outcome of not only how animals use resources, but of  
635 the tempo and fidelity of isotopic incorporation. These are shaped by the mechanisms by which animals incorporate and dispose materials into their tissues. We believe that incorporating these mechanisms into dynamic models can transform isotopic ecology from a descriptive into a more dynamic process-based discipline. Recent studies advocated for the use of simulation modelling to predict stable isotope ratios using mechanistic processes (e.g.  
640 Flynn et al. 2018; Trueman et al. 2019). IsoDyn model can be an element of these models, and hence can be a further step in the direction of a mechanistic process-based isotopic ecology.

## Declaration

645 Funding: This study is part of the ISIT-U project which was supported by the French government through the Programme Investissement d'Avenir (I-SITE ULNE / ANR-16-IDEX-0004 ULNE) managed by the Agence Nationale de la Recherche and the métropole Européenne de Lille.

Code and data availability: R code for all analyses, figures and tables is available from

650 GitHub (<https://github.com/Sebastien-Lefebvre/IsoDyn>)

Conflict of interest: The authors declare that they have no conflict of interest

Ethical approval: This article does not contain any studies with human participants or animals performed by any of the authors

655

## References

Boecklen WJ, Yarnes CT, Cook BA, James AC (2011) On the use of stable isotopes in trophic ecology. *Annu Rev Ecol Evol Syst* 42:411-440. doi: 10.1146/annurev-ecolsys-102209-144726

660 Carleton SA, Martinez del Rio C (2010) Growth and catabolism in isotopic incorporation: a new formulation and experimental data. *Funct Ecol* 24:805-812. doi: 10.1111/j.1365-2435.2010.01700.x

Carter WA, Bauchinger U, McWilliams SR (2019) The importance of isotopic turnover for understanding key aspects of animal ecology and nutrition. *Diversity* 11. doi: 10.3390/d11050084

665 Caut S, Angulo E, Courchamp F (2009) Variation in discrimination factors ( $\Delta^{15}\text{N}$  and  $\Delta^{13}\text{C}$ ): the effect of diet isotopic values and applications for diet reconstruction. *J Appl Ecol* 46:443-453. doi: 10.1111/j.1365-2664.2009.01620.x

Dalerum F, Angerbjorn A (2005) Resolving temporal variation in vertebrate diets using naturally occurring stable isotopes. *Oecologia* 144:647-658. doi: 10.1007/s00442-005-0118-0

670 De Niro MJ, Epstein S (1978) Influence of diet on the distribution of carbon isotopes in animals. *Geochim Cosmochim Ac* 42:495-506. doi: doi.org/10.1016/0016-7037(78)90199-0

Emmery A, Lefebvre S, Alunno-Bruscia M, Kooijman SALM (2011) Understanding the dynamics of  $\delta^{13}\text{C}$  and  $\delta^{15}\text{N}$  in soft tissues of the bivalve *Crassostrea gigas* facing environmental fluctuations in the context of Dynamic Energy Budgets (DEB). *J Sea Res* 66:361-371. doi: 10.1016/j.seares.2011.08.002

675 Fink P, Reichwaldt ES, Harrod C, Rossberg AG (2012) Determining trophic niche width: an experimental test of the stable isotope approach. *Oikos* 121:1985-1994. doi: 10.1111/j.1600-0706.2012.20185.x

680 Flynn KJ, Mitra A, Bode A (2018) Toward a mechanistic understanding of trophic structure: inferences from simulating stable isotope ratios. *Mar Biol* 165:147. doi: 10.1007/s00227-018-3405-0

Fry B, Arnold C (1982) Rapid C-13/C-12 turnover during growth of brown shrimp (*Penaeus aztecus*). *Oecologia* 54:200-204. doi: 10.1007/bf00378393

685 Gaye-Siessegger J, Focken U, Muetzel S, Abel H, Becker K (2004) Feeding level and individual metabolic rate affect  $\delta^{13}\text{C}$  and  $\delta^{15}\text{N}$  values in carp: implications for food web studies. *Oecologia* 138:175-183. doi: 10.1007/s00442-003-1429-7

Glibert PM, Middelburg JJ, McClelland JW, Jake Vander Zanden M (2018) Stable isotope tracers: Enriching our perspectives and questions on sources, fates, rates, and pathways of major elements in aquatic systems. *Limnol Oceanogr* 64:950-981. doi: 10.1002/lno.11087

690 Gorokhova E (2018) Individual growth as a non-dietary determinant of the isotopic niche metrics. *Methods Ecol Evol* 9:269-277. doi: 10.1111/2041-210x.12887

Guelinckx J, Maes J, Van Den Driessche P, Geysen B, Dehairs F, Ollevier F (2007) Changes in  $\delta^{13}\text{C}$  and  $\delta^{15}\text{N}$  in different tissues of juvenile sand goby *Pomatoschistus minutus*: a laboratory diet-switch experiment. *Mar Ecol Prog Ser* 341:205-215

695 Healy K, Guillerme T, Kelly SBA, Inger R, Bearhop S, Jackson AL (2018) SIDER: an R package for predicting trophic discrimination factors of consumers based on their ecology and phylogenetic relatedness. *Ecography* 41:1393-1400. doi: 10.1111/ecog.03371

Hertz E et al. (2016) Hitting the moving target: modelling ontogenetic shifts with stable isotopes reveals the importance of isotopic turnover. *J Anim Ecol* 85:681-691. doi: 10.1111/1365-2656.12504

700 Hesslein RH, Hallard KA, Ramlal P (1993) Replacement of sulfur, carbon, and nitrogen in tissue of growing broad whitefish (*Coregonus nasus*) in response to a change in diet traced by  $\delta^{34}\text{S}$ ,  $\delta^{13}\text{C}$ , and  $\delta^{15}\text{N}$ . *Can J Fish Aquat Sci* 50:2071-2076. doi: 10.1139/f93-230

Hou C, Bolt KM, Bergman A (2011) A general model for ontogenetic growth under food restriction. *Proc R Soc B-Biol Sci* 278:2881-2890. doi: 10.1098/rspb.2011.0047

Hussey NE et al. (2014) Rescaling the trophic structure of marine food webs. *Ecol Lett* 17:239-250. doi: 10.1111/ele.12226

Kadoya T, Osada Y, Takimoto G (2012) IsoWeb: a Bayesian isotope mixing model for diet analysis of the whole food web. *PLoS One* 7:e41057. doi: 10.1371/journal.pone.0041057

710 Kearney MR (2020) What is the status of metabolic theory one century after Putter invented the von Bertalanffy growth curve? *Biol Rev Camb Philos Soc.* doi: 10.1111/brv.12668

Kooijman SALM (2010) Dynamic energy budget theory for metabolic organisation. Cambridge University Press, Cambridge, UK

715 Layman CA et al. (2012) Applying stable isotopes to examine food-web structure: an overview of analytical tools. *Biol Rev* 87:545-562. doi: 10.1111/j.1469-185X.2011.00208.x

Lefebvre S, Dubois SF (2016) The stony road to understand isotopic enrichment and turnover rates: insight into the metabolic part. *Vie Milieu* 66:305-314

720 Logan JM, Lutcavage ME (2010) Stable isotope dynamics in elasmobranch fishes. *Hydrobiologia* 644:231-244. doi: 10.1007/s10750-010-0120-3

725 MacAvoy SE, Macko SA, Arneson LS (2005) Growth versus metabolic tissue replacement in mouse tissues determined by stable carbon and nitrogen isotope analysis. *Can J Zool* 83:631-641. doi: 10.1139/z05-038

Marín Leal JC et al. (2008) Stable isotopes ( $\delta^{13}\text{C}$ ,  $\delta^{15}\text{N}$ ) and modelling as tools to estimate the trophic ecology of cultivated oysters in two contrasting environments. *Mar Biol* 153:673-688. doi: 10.1007/s00227-007-0841-7

730 Marques GM, Augustine S, Lika K, Pecquerie L, Domingos T, Kooijman SALM (2018) The AmP project: Comparing species on the basis of dynamic energy budget parameters. *PLoS Comput Biol* 14:e1006100. doi: 10.1371/journal.pcbi.1006100

735 Marques GM, Lika K, Augustine S, Pecquerie L, Kooijman SALM (2019) Fitting multiple models to multiple data sets. *J Sea Res* 143:48-56. doi: 10.1016/j.seares.2018.07.004

Martinez Del Rio C, Anderson-Sprecher R (2008) Beyond the reaction progress variable: the meaning and significance of isotopic incorporation data. *Oecologia* 156:765-772. doi: 10.1007/s00442-008-1040-z

740 Martinez del Rio C, Carleton SA (2012) How fast and how faithful: the dynamics of isotopic incorporation into animal tissues. *J Mammal* 93:353-359. doi: 10.1644/11-mamm-s-165.1

Martinez del Rio C, Wolf BO (2005) Mass-balance models for animal isotopic ecology. In: Starck JM, Wang T (eds) *Physiological and Ecological Adaptations to Feeding In Vertebrates*. Science publishers, Enfield, New Hampshire, pp 141-174

745 Martinez del Rio C, Wolf N, Carleton SA, Gannes LZ (2009) Isotopic ecology ten years after a call for more laboratory experiments. *Biol Rev* 84:91-111. doi: 10.1111/j.1469-185X.2008.00064.x

McCutchan JH, Lewis WM, Kendall C, McGrath CC (2003) Variation in trophic shift for stable isotope ratios of carbon, nitrogen, and sulfur. *Oikos* 102:378-390. doi: 10.1034/j.1600-0706.2003.12098.x

Nahon S, Séité S, Lefebvre S, Kolasinski J, Aguirre P, Geurden I (2020) How protein quality drives 750 incorporation rates and trophic discrimination of carbon and nitrogen stable isotope ratios in a freshwater first-feeding fish. *Freshw Biol* 65:1870-1882. doi: 10.1111/fwb.13578

Nakazawa T et al. (2010) Is the relationship between body size and trophic niche position time-invariant in a predatory fish? First stable isotope evidence. *Plos One* 5:e0009120. doi: 10.1371/journal.pone.0009120

Nuche-Pascual MT, Lazo JP, Ruiz-Cooley RI, Herzka SZ (2018) Amino acid-specific  $\delta^{15}\text{N}$  trophic enrichment factors in fish fed with formulated diets varying in protein quantity and quality. *Ecol Evol* 8:9192-9217. doi: 10.1002/ece3.4295

Olive PJW, Pinnegar JK, Polunin NVC, Richards G, Welch R (2003) Isotope trophic-step fractionation: a dynamic equilibrium model. *J Anim Ecol* 72:608-617. doi: 10.1046/j.1365-2656.2003.00730.x

755 Parnell AC, Inger R, Bearhop S, Jackson AL (2010) Source partitioning using stable isotopes: Coping with too much variation. *Plos One* 5. doi: 10.1371/journal.pone.0009672

Parnell AC et al. (2013) Bayesian stable isotope mixing models. *Environmetrics* 24:387-399. doi: 10.1002/env.2221

Pecquerie L, Nisbet RM, Fablet R, Lorrain A, Kooijman SA (2010) The impact of metabolism on stable isotope dynamics: a theoretical framework. *Philos Trans R Soc B-Biol Sci* 365:3455-3468. doi: 10.1098/rstb.2010.0097

Phillips DL et al. (2014) Best practices for use of stable isotope mixing models in food-web studies. *Can J Zool* 92:823-835. doi: 10.1139/cjz-2014-0127

Post DM (2002) The long and short of food-chain length. *Trends Ecol Evol* 17:269-277. doi: 10.1016/s0169-5347(02)02455-2

760 Poupin N, Mariotti F, Huneau JF, Hermier D, Fouillet H (2014) Natural isotopic signatures of variations in body nitrogen fluxes: a compartmental model analysis. *PLoS Comput Biol* 10:e1003865. doi: 10.1371/journal.pcbi.1003865

765 Quezada-Romegialli C et al. (2018) tRophicPosition , an R package for the Bayesian estimation of trophic position from consumer stable isotope ratios. *Methods Ecol Evol* 9:1592-1599. doi: 10.1111/2041-210x.13009

Shipley ON, Matich P (2020) Studying animal niches using bulk stable isotope ratios: an updated synthesis. *Oecologia* 193:27-51. doi: 10.1007/s00442-020-04654-4

770 Soetaert K, Petzoldt T, Setzer RW (2010) Solving differential equations in R. *The R Journal* 2:5-15

775 Stock BC, Semmens BX (2016) Unifying error structures in commonly used biotracer mixing models. *Ecology* 97:2562-2569

Thomas SM, Crowther TW (2015) Predicting rates of isotopic turnover across the animal kingdom: a synthesis of existing data. *J Anim Ecol* 84:861-870. doi: 10.1111/1365-2656.12326

Tieszen LL, Boutton TW, Tesdahl KG, Slade NA (1983) Fractionation and turnover of stable carbon 780 isotopes in animal tissues: implications for  $\delta^{13}\text{C}$  analysis of diet. *Oecologia* 57:32-37. doi: 10.1007/bf00379558

Trueman CN et al. (2019) Combining simulation modeling and stable isotope analyses to reconstruct the last known movements of one of Nature's giants. *PeerJ* 7:e7912. doi: 10.7717/peerj.7912

Vander Zanden JM, Fetzer W (2007) Global patterns of aquatic food chain length. *Oikos* 116:1378-785 1388. doi: 10.1111/j.0030-1299.2007.16036.x

Vander Zanden MJ, Clayton MK, Moody EK, Solomon CT, Weidel BC (2015) Stable isotope turnover and half-life in animal tissues: a literature synthesis. *PLoS One* 10:e0116182. doi: 10.1371/journal.pone.0116182

790 Vander Zanden MJ, Rasmussen JB (2001) Variation in  $\delta^{15}\text{N}$  and  $\delta^{13}\text{C}$  trophic fractionation: Implications for aquatic food web studies. *Limnol Oceanogr* 46:2061-2066

Vanderklift MA, Ponsard S (2003) Sources of variation in consumer-diet  $\delta^{15}\text{N}$  enrichment: a meta-analysis. *Oecologia* 136:169-182. doi: 10.1007/s00442-003-1270-z

Villamarín F, Jardine TD, Bunn SE, Marioni B, Magnusson WE (2018) Body size is more important than diet in determining stable-isotope estimates of trophic position in crocodilians. *Sci Rep* 795 8:2020. doi: 10.1038/s41598-018-19918-6

Von Bertalanffy L (1957) Quantitative laws in metabolism and growth. *Q Rev Biol* 32:217-231. doi: 10.1086/401873

West GB, Brown JH, Enquist BJ (2001) A general model for ontogenetic growth. *Nature* 413:628-631. doi: 10.1038/35098076

800 Yeakel JD, Bhat U, Elliott Smith EA, Newsome SD (2016) Exploring the isotopic niche: isotopic Variance, physiological incorporation, and the temporal dynamics of foraging. *Front Ecol Evol* 4. doi: 10.3389/fevo.2016.00001

Table 1 List of abbreviations and symbols used throughout the manuscript

Abreviation or symbol	Unit	Definition
$\delta$ or $\delta^H X$	‰	The ratio of heavy (H) to light isotope in element X in $\delta$ notation Noted $\delta$ for sake of simplicity in some occasion
$\Delta$ or $\Delta^H X$	‰	The trophic discrimination factor i.e. the difference in $\delta$ value between the $\delta$ value of the consumer and the $\delta$ value its diet Received a variety of names depending on the application including trophic shift (e.g. McCutchan et al. 2003), trophic fractionation (Vander Zanden and Rasmussen 2001), trophic enrichment factor (Post 2002) diet to tissue discrimination factor (Hussey et al. 2014). Noted $\Delta$ for sake of simplicity in some occasion
$\lambda$	$d^{-1}$	The isotopic incorporation rate also named the isotopic turnover rate with the interpretation of $1/\lambda$ as the average retention time of an element in a tissue, and $\ln(2)/\lambda$ as its half-life (Thomas et al. 2015; Vander Zanden et al. 2015)
$\delta_\infty$	‰	Asymptotic value of $\delta$ in the time model of isotopic incorporation needed to calculate $\Delta$
$k_g$	$d^{-1}$	The specific growth rate in an exponential model (also noted k). Net addition of new tissues
$k_c$	$d^{-1}$	Catabolic turnover rate also noted k or m and named metabolic turnover rate. Renewal of old tissues
W	g	Body mass or wet weight
$W_\infty$	g	Asymptotic body mass
$r_i$	$g^{1-\beta} d^{-1}$	Rate of body mass gains (or inputs). Named anabolic rate in von Bertalanffy growth model or Ontogenetic growth model and assimilation rate in DEB Theory. Note that underlying mechanisms may differ (Kearney 2020).
$r_o$	$d^{-1}$	Rate of body mass losses (or outputs). Named catabolic rate in von Bertalanffy growth model and maintenance rate in DEB Theory or Ontogenetic growth model. Note that underlying mechanisms may differ (Kearney 2020)
$\beta$	-	Allometric coefficient
$\Delta_i$	‰	Isotopic discrimination on the flux of body mass gains
$\Delta_o$	‰	Isotopic discrimination on the flux of body mass losses
DIIM		Models of the dynamics of isotope incorporation in consumer tissues as a function of time or body mass. Usually one compartment first order kinetics assuming exponential growth of the consumer of which the time model (Tieszen et al. 1983; Heisslein et al. 1993) or the mass model (Carleton and Martinez Del Rio 2010)
DSE	-	Diet switch(ing) experiment. A controlled experiment in which a switch in diet is provoked while $\delta$ values of the consumers are measured over time and potentially body mass dynamics
RE	%	Relative error. Used to assess the goodness of fit of the models

Table 2 Parameter estimation (best estimates and interval estimates) of the two isotopic incorporation approaches: (1) the time model assuming exponential growth, TIM; (2) the IsoDyn model assuming asymptotic growth patterns with an allometric coefficient  $\beta=2/3$  for the three case studies. Interval estimates are 95% confidence interval for TIM, and 2.5% and 97.5% quantiles for Isodyn as parameter interval density distribution did not follow a normal distribution. Relative Error (RE, %) between observations and predictions for the body mass and the  $\delta^{15}\text{N}$  values, and the mean RE between the two latter. Specific parameters of Isodyn model are  $r_i$  (rate of gains or assimilation),  $r_o$  (rate of losses or excretion equivalent to the catabolic rate  $k_c$ ),  $\Delta_i$  and  $\Delta_o$  (isotopic discrimination on gains and losses respectively) related to eq(8). In Isodyn model, the isotopic incorporation rate ( $\lambda$ ), the specific growth rate ( $k_g$ ) and the asymptotic trophic discrimination factor ( $\Delta^{15}\text{N}$ ) are calculated following eq (7), eq (10), and as  $\Delta_i - \Delta_o$  respectively. Specific parameters of the time model are  $\lambda$ ,  $\Delta^{15}\text{N}$ ,  $k_g$  and  $k_c$  related to eq (1 to 4). Standard propagation of error formulae were used to estimate interval of parameters not directly estimated from the fitting methods

Study	Parameter	Units	Estimates (interval)	
			IsoDyn model	Time model
<b>Pacific yellowtail</b> Nuche et al. (2018)	RE body mass	%	12.5	19.1
	RE $\delta^{15}\text{N}$	%	1.1	1.2
	Mean RE	%	6.8	10.1
	$r_i$	$\text{g}^{1/3} \text{d}^{-1}$	21.03 (15.70 - 26.86) $10^{-2}$	-
	$r_o$ or $k_c$	$\text{d}^{-1}$	3.04 (1.88 - 4.27) $10^{-2}$	3.04 (1.90 - 4.17) $10^{-2}$
	$k_g$	$\text{d}^{-1}$	1.83 (1.65 - 1.99) $10^{-2}$	2.18 (2.14 - 2.22) $10^{-2}$
	$\Delta_i - \Delta_o$	‰	1.28 (1.16 - 1.43)	-
	$\lambda$	$\text{d}^{-1}$	4.87 (3.58 - 6.24) $10^{-2}$	5.21 (3.09 - 7.34) $10^{-2}$
	$\Delta^{15}\text{N}$	‰	2.55 (2.33 - 2.85)	2.12 (1.94 - 2.29)
<b>Adult mouse</b> MacAvoy et al. (2005)	$k_g/\lambda$	%	37.5	41.8
	RE body mass	%	2.0	3.4
	RE $\delta^{15}\text{N}$	%	0.9	1.0
	Mean RE	%	1.5	2.2
	$r_i$	$\text{g}^{1/3} \text{d}^{-1}$	11.16 (4.77 - 50.0) $10^{-2}$	-
	$r_o$ or $k_c$	$\text{d}^{-1}$	3.86 (1.57 - 18.0) $10^{-2}$	3.03 (1.76 - 4.30) $10^{-2}$
	$k_g$	$\text{d}^{-1}$	0.24 (0.14 - 0.32) $10^{-2}$	0.27 (0.21 - 0.33) $10^{-2}$
	$\Delta_i - \Delta_o$	‰	1.32 (1.05 - 1.94)	-
	$\lambda$	$\text{d}^{-1}$	4.10 (1.75 - 18.34) $10^{-2}$	3.27 (1.57 - 5.03) $10^{-2}$
<b>Sand goby</b> Guelinkx et al. (2007)	$\Delta^{15}\text{N}$	‰	2.64 (2.11 - 3.88)	1.70 (1.29 - 2.11)
	$k_g/\lambda$	%	5.9	8.3
	RE body mass	%	9.3	9.4
	RE $\delta^{15}\text{N}$	%	1.8	1.7
	Mean RE	%	5.5	5.6
	$r_i$	$\text{g}^{1/3} \text{d}^{-1}$	1.77 (1.27-8.07) $10^{-2}$	-
	$r_o$ or $k_c$	$\text{d}^{-1}$	0.71 (0.57-6.16) $10^{-2}$	1.59 (0.81-2.36) $10^{-2}$
	$k_g$	$\text{d}^{-1}$	0.87 (0.53-1.27) $10^{-2}$	0.87 (0.77-0.96) $10^{-2}$
	$\Delta_i - \Delta_o$	‰	2.05 (1.41-2.63)	-

Table 3 Estimates of scaled functional response (f), a Holling type II functional response ranging from 0 to 1, of the von Bertalanffy model as predicted by DEB theory (see supplementary material 2 for details) and related  $r_i$  (rate of gains i.e. assimilation) and  $r_o$  (rate of losses i.e. excretion) values from the Common carp case study (Gaye-Siesseger et al. 825 2004). Fish were fed at four feeding ration levels (L) from the lowest feeding ration levels to the highest ones (1 to 4)

Feeding ration level	f (unitless)	$r_i$ ( $\text{g}^{1/3} \text{ d}^{-1}$ )	$r_o$ ( $\text{d}^{-1}$ )
L 1	0.16	$7.39 \cdot 10^{-2}$	$2.27 \cdot 10^{-2}$
L 2	0.29	$9.62 \cdot 10^{-2}$	$1.37 \cdot 10^{-2}$
L 3	0.53	$12.34 \cdot 10^{-2}$	$0.78 \cdot 10^{-2}$
L 4	0.82	$14.47 \cdot 10^{-2}$	$0.52 \cdot 10^{-2}$

830

## Figure Legends

Fig. 1 Main features of the IsoDyn model compared to the conventional time model of isotope incorporation (Hesslein et al. 1993). IsoDyn model accounts for many growth forms and offers new perspective in the interpretation of diet switch experiments (DSE) and dynamics of 835 isotope incorporation into animal tissues in general

Fig. 2 General patterns of the IsoDyn model over time for three virtual species (see text for details) with an allometric coefficient  $\beta = 2/3$ . The same parameters that shape growth also shape isotopic incorporation. A) Body mass over time B) Range of values of isotopic 840 incorporation rate  $\ln(\lambda) = \ln(r_i) + (\beta-1) \ln(W)$ , C)  $\delta^{15}\text{N}$  difference between body and diet as a function of specific growth rate ( $k_g$ ) with  $\Delta_i = 2\text{‰}$ ,  $\Delta_o = -2\text{‰}$  and  $\delta^{15}\text{N}_d = 0\text{‰}$ .  $k_g$  was calculated following eq(15)

Fig. 3 Typical 100-day Diet Switch Experiment for three species with different growth 845 patterns (described in text and Fig. 2) and comparing patterns for juveniles and adults. Figures describe changes in  $\delta^{15}\text{N}_b$  of whole body over time for Sp1, Sp2, and Sp3. In each species, the experiment for juveniles starts at  $W_0$ . For adults, experiments start at  $W_{\max}$ . The dash line represents  $\delta^{15}\text{N}_d$  value of the new diet

850 Fig. 4 Changes in body mass (in g; left column) and  $\delta^{15}\text{N}_m$  values of muscle tissue (in ‰; right column) in three species (young adult mouse *Mus musculus* data from MacAvoy et al. 2005; Pacific yellowtail juvenile fish *Seriola lalandi* data from Nuche-Pascual et al. 2018; sand goby juvenile fish *Pomatoschistus minutus* data from Guelinckx et al. 2007). Open circles are observations (mean  $\pm$  sd), solid lines are predictions from Isodyn model (eq 6 and 855 13), dotted lines are predictions from the time model (eq 1 and 4). Colored envelopes are 2.5 and 97.5 quantiles of IsoDyn model predictions. Grey dashed lines are  $\delta^{15}\text{N}_d$  of the new diet

Fig. 5 Changes in body mass (A) and  $\delta^{15}\text{N}_b$  values of whole body minus  $\delta^{15}\text{N}_d$  values of the diet (B) in common carp (*Cyprinus carpio*) diet-shifted to a new diet and fed four different 860 feeding ration levels (L1, L2, L3, L4; Gaye-Siesseger et al. 2004). Closed circles are observations and lines are predictions. C) represents  $\delta^{15}\text{N}_b - \delta^{15}\text{N}_d$  for each diet and hence for each mass specific growth rates

Fig. 1

865

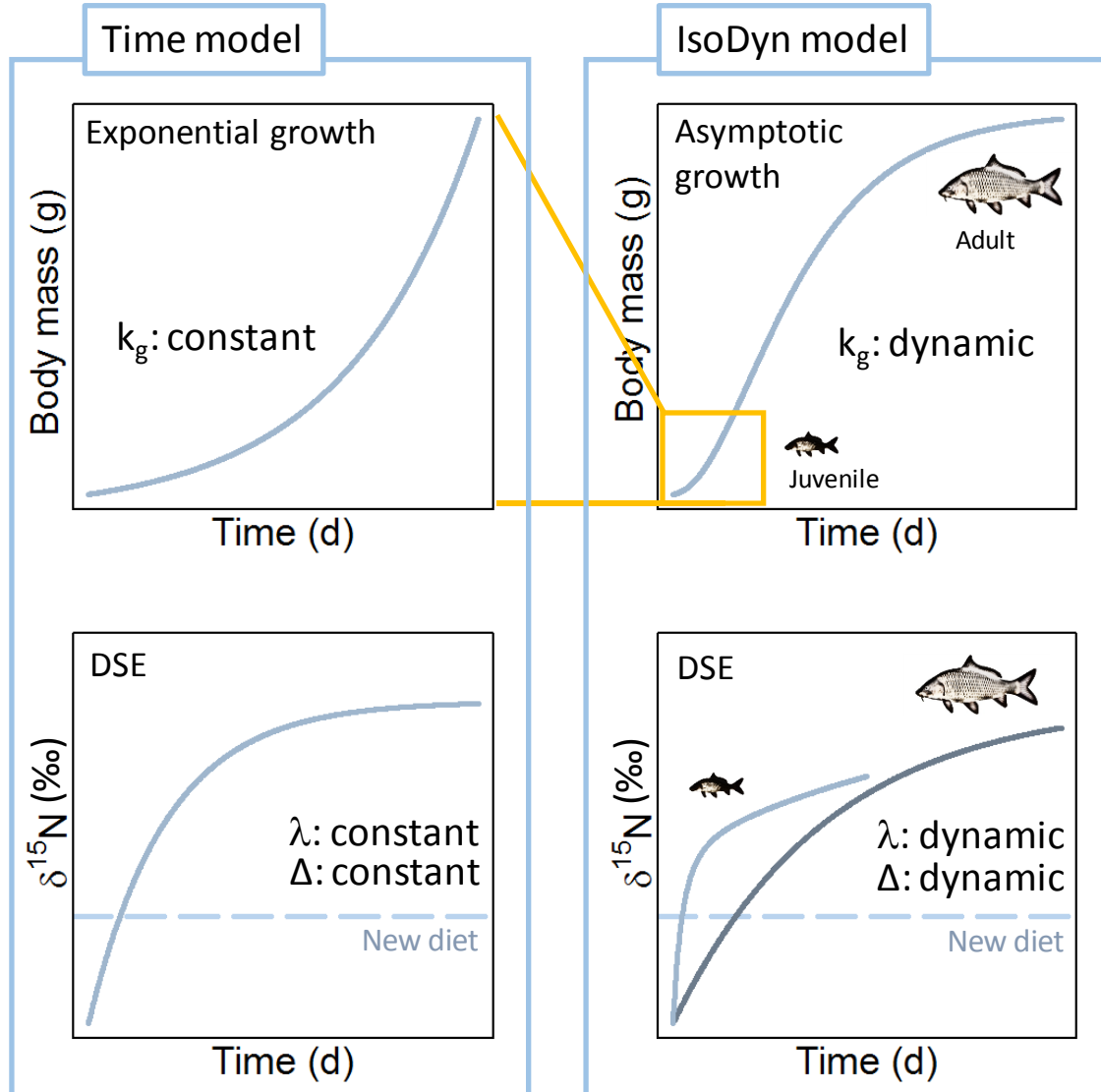


Fig. 2

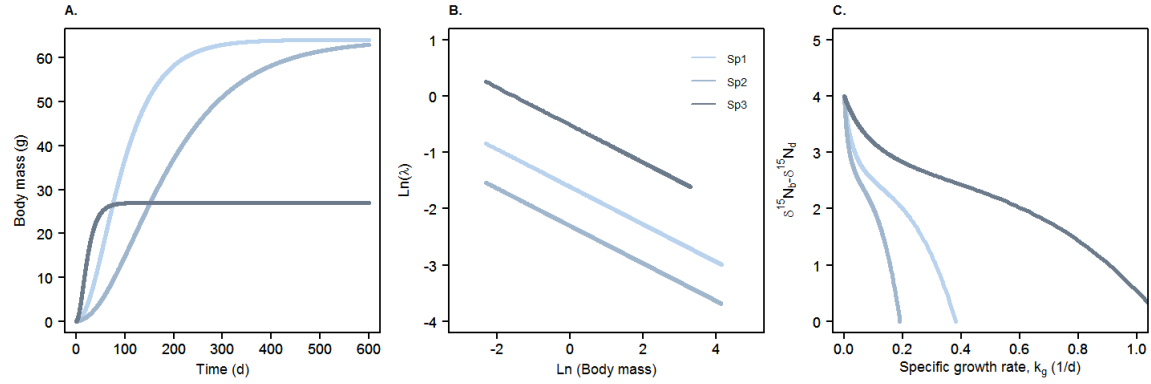


Fig. 3

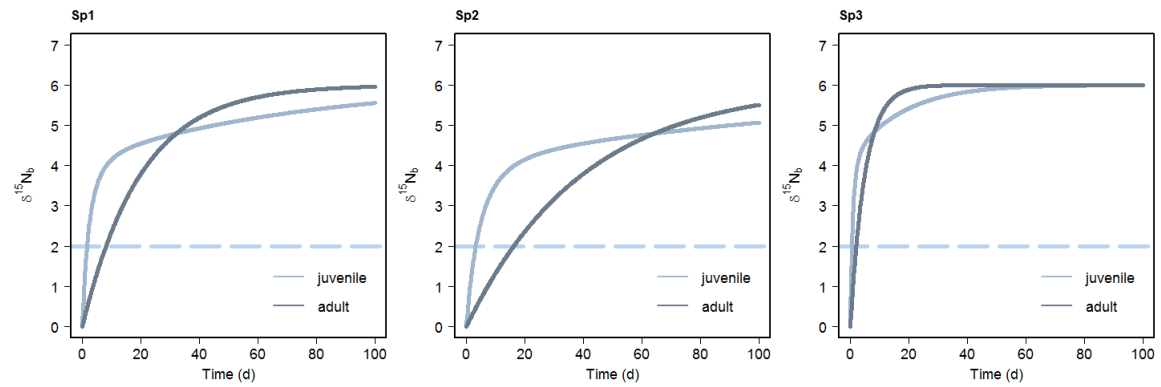
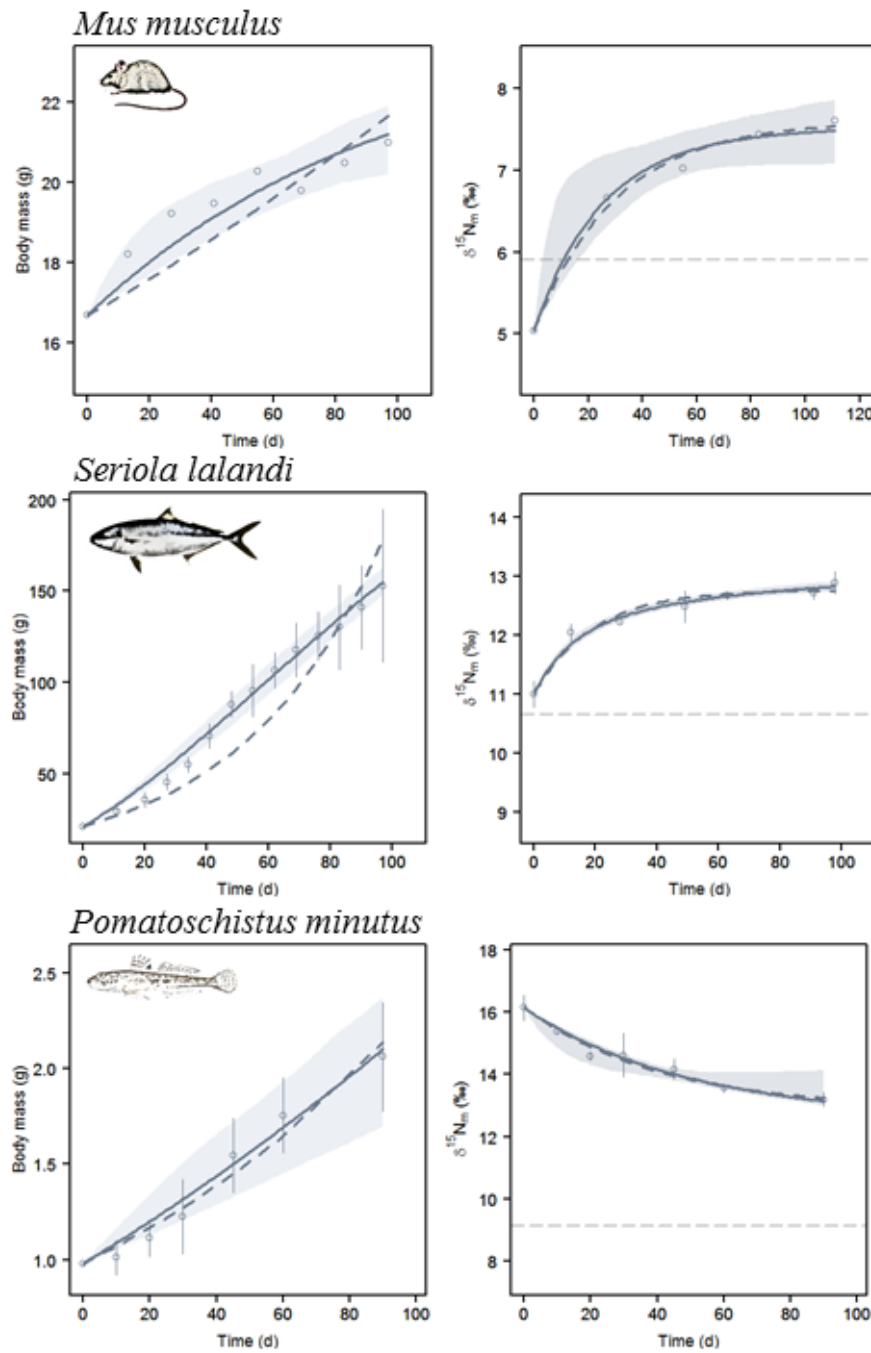


Fig. 4



880 Fig. 5

